DEEP FABRY-PEROT IMAGING OF NGC 6240: KINEMATIC EVIDENCE FOR MERGING GALAXIES

J. Bland Hawthorn
Dept. of Space Physics and Astronomy, Rice University, Houston, TX 77251-1892

A. S. Wilson
Astronomy Program, University of Maryland, College Park, MD 20742

R. B. Tully
Institute for Astronomy, Honolulu, Hawaii 96822

ABSTRACT. We have observed the superluminous, infrared galaxy NGC 6240 ($z = 0.025$) at Hα with the Hawaii Imaging Fabry-Perot Interferometer (HIFI - Bland and Tully 1989). During the past decade, observational evidence from all wavebands indicates that the unusual appearance of NGC 6240 has resulted from a collision between two gas-rich systems, a view which is supported by our spectrophotometric data. However, the origin of the enormous infrared luminosity (4×10^{11} L_0) detected by IRAS remains highly controversial, where opinions differ on the relative roles of large-scale shocks, massive star formation or a buried "active" nucleus. These mechanisms are discussed in the light of our Fabry-Perot observations.

OBSERVATIONS

The HIFI system was mounted at the Cassegrain focus of the University of Hawaii 2.2m telescope. We observed 12 frames for a total of six hours at 68 km s^{-1} increments across the Hα line, which is comparable to the spectral resolution of the high finesse (60) etalon, providing a velocity coverage of 820 km s^{-1}. A low read-noise (~4e$^-$), 385 $\times$ 576 format GEC CCD was placed at the image plane. The f/2 input beam yielded an angular resolution of 0.85" per pixel providing an overall field-of-view of 8' by 5'. These observations have been supplemented with Hα, [OIII]λ5007 and Hβ narrowband imagery using the Prime Focus CCD at the CTIO 4m telescope. The RCA 512 $\times$ 320 CCD has an angular resolution of 0.60" per pixel providing an overall field-of-view of 5' $\times$ 3'. The total integration time for each on-band and off-band image is 1200s. The thinned chip has fringing problems that are largely divided out using flatfields except for the Hα observation where a dome flat was not taken. Charge transfer "bleeding" about bright stars has been removed using row-oriented, sinc interpolation. The normal stages of photometric calibration (bias and sky subtraction, relative scaling with field stars, etc.) have been applied to all images, the results of which are shown in Figs. 1 and 2.

RESULTS

Fosbury and Wall (1979) first drew attention to the unusual appearance of NGC 6240: their photographic plates taken at the ESO 3.6m telescope showed clearly a number of plumes extending in all directions from a bright, central region. Fig. 1(a) shows an optical continuum image that exhibits all of these features. Fosbury and Wall suggested that most of the flux arising from the central region is line emission, a supposition that is confirmed by the Hα and [OIII]λ5007 images in Figs. 2(a) and 2(b) respectively. Even with the limited velocity coverage of the Fabry-Perot spectra, a comparison of the integrated line emission shown in Fig. 3(a) with Fig. 2(a) and the imagery of Heckman, Armus and Miley (1987) demonstrates that we detect most of the Hα flux to the limits of these CCD images ($\approx 6 \times 10^{-17}$ erg cm^{-2} s^{-1} arcsec^{-2}). However, in a few specific locations, there is some confusion between line and continuum in that these are indistinguishable in the HIFI data for lines broader than 600 km s^{-1} FWHM. Indeed, the HIFI data show that the bright inner region is dominated by emission with line

https://doi.org/10.1017/S0252921100005480 Published online by Cambridge University Press

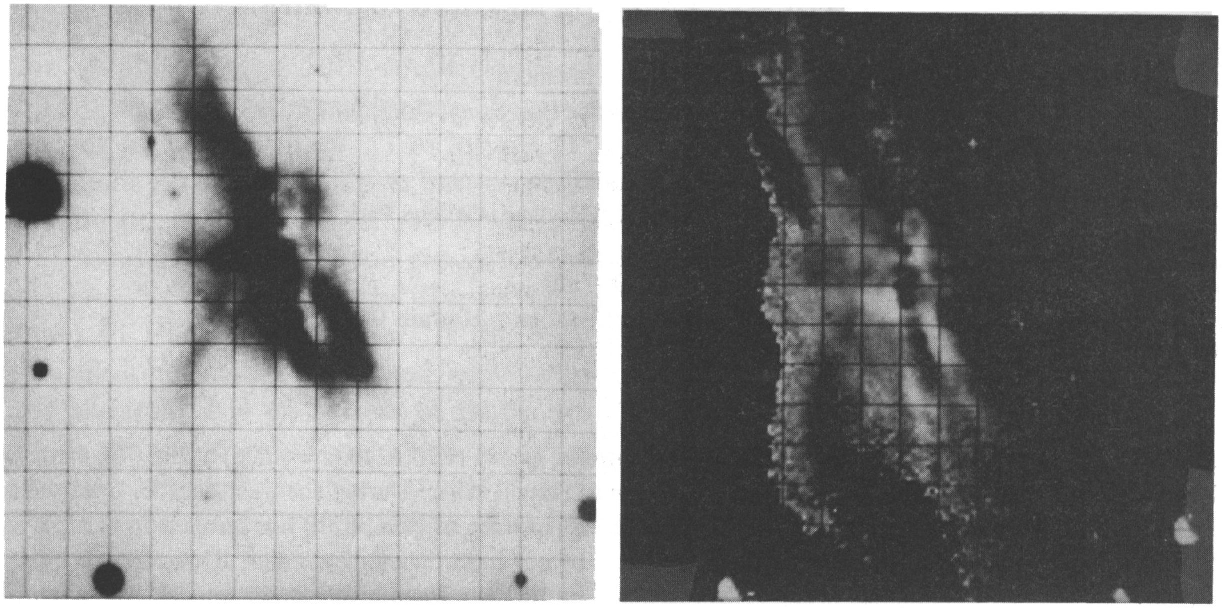

Figure 1(a). An optical continuum image of NGC 6240 formed from the sum of two images taken through 100Å filters, centered at λ5400 and λ7080, using the Prime Focus CCD at the CTIO 4m telescope. For all plates, the field-of-view shown is 90" × 90" where north is upwards and east is to the left. The grid lines are spaced at 6" intervals along both axes to aid comparisons between the figures. (b). An image formed from the ratio of the two continuum images used in (a). Light and dark areas show regions of relatively high and low extinction. The double nucleus, seen at the center of the image, occurs along one of the low extinction bands.

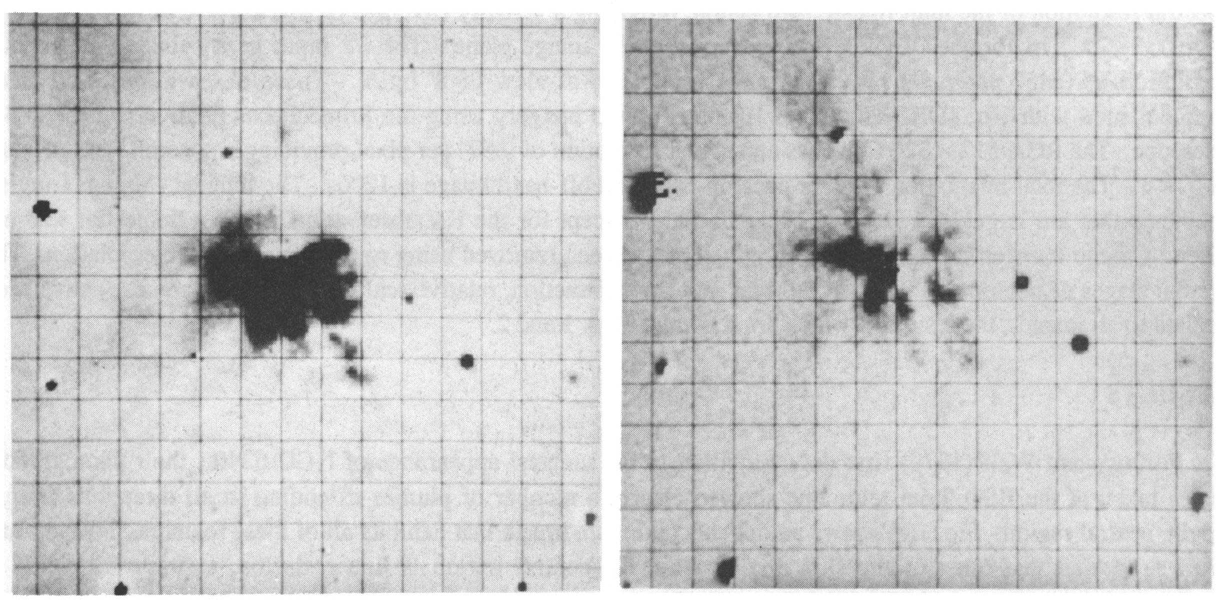

Figure 2(a). The Hα line flux distribution in the central regions of NGC 6240 obtained from on-band/off-band imaging with the CTIO Prime Focus CCD. The fringes arise from night-sky lines within the filter bandpass. (b). The [OIII]λ5007 line flux distribution in the central regions of NGC 6240. Notice the residuals from the double nuclei resemble the residuals from the field stars. The two HII regions to the west are roughly a magnitude brighter in [OIII]λ5007 than in Hα.

https://doi.org/10.1017/S0252921100005480 Published online by Cambridge University Press

widths ~1000 km s^{-1} FWHM. Long-slit spectra covering the wavelength range λ4200-λ5300 taken at the CTIO 4m telescope confirm this same behavior in the [OIII]λ5007 line emission. Moreover, both the Hα and the [OIII]λ5007 line profiles are observed to broaden as the flux within the line increases (see also Keel, this conference).

Figure 1(b) shows the ratio of the off-band continuum images centered at λ5400 and λ7080 and serves to illustrate regions of relatively low (dark) and high (light) dust extinction. Parallel strands of low and high extinction are observed to run from NE to SW with the SE plume exhibiting a similar behavior. The resolved double nucleus, first identified at radio (Condon et al. 1982) and optical wavelengths (Fried and Schulz 1983) is easily seen in the center of the image and lies along a strand of relatively low extinction. The ratio of the Hβ to Hα line flux images confirms our interpretation of Fig. 1(b). While the [OIII]λ5007/Hα ratio tracks the Hβ/Hα ratio rather closely, the imagery was not considered to be good enough to correct the [OIII]λ5007 flux for extinction effects. Over the bright inner region, the Hβ/Hα ratio implies a magnitude of extinction between these wavelengths favoring a visual extinction, $A_V \approx$ 3-4 mag and a total Hα luminosity, $L_{H\alpha} \sim 5 \times 10^{42}$ erg s^{-1}.

The Fabry-Perot data and Fig. 2(a) demonstrate that the line emission separates into at least three distinct components: (i) several filamentary "arms" that extend across the entire field-of-view, (ii) a diffuse envelope with dimensions 80" × 50" whose long axis is aligned with the long axis of the galaxy, which encompasses (iii) a luminous "spur" ($L_{H\alpha} \sim 2 \times 10^{41}$ $ergs^{-1}$) that extends 20" SW from the double nucleus. There is marginal evidence for a limb-brightened "bubble" 35" due north of the nucleus as only in this region are narrow spectral lines observed to split with a maximum separation of ~350 km s^{-1}. The bow-shock morphology is similar to the bipolar bubbles in M82 (Bland and Tully 1988) although the distance to NGC 6240 (98 Mpc) makes this feature much larger (~17 kpc).

The HIFI spectra show that while the Hα line profiles are both broad and display complex structure over the inner region, all profiles exhibit a bright component that dominates the line emission. These have been fitted with gaussians and the resultant velocity field is presented in Fig. 3(b). While the velocity field appears complicated, large-scale patterns do emerge. The gross distribution of the line flux in Fig. 3(a) can be described in terms of two axes, one that runs from SW to NE through the double radio source (Axis 1), and another that crosses the top of the latter from SE to NW (Axis 2). Both of these directions define the steepest gradients through the velocity field. Along Axis 1, the gradient is ~300 km s^{-1} over about 15" centered on the double nucleus, turning over in both directions outside of this range. The gradient along Axis 2 is much steeper at ~500 km s^{-1} over about 5" centered on a point 10" NE of the compact radio source. If the latter defines the systemic velocity, the second system is redshifted by only 70 km s^{-1} with respect to the nucleus. A preliminary interpretation (Bland, Wilson and Tully, in prep.) suggests that the velocity field may be explained in terms of two rotating discs that are only 5 kpc apart in projection, as illustrated by the two ellipses in Fig. 3(b).

PRELIMINARY INTERPRETATION

Evidence for an "active" nucleus. The idea of a buried AGN was originally proposed to explain the non-thermal spectrum of the compact, double radio source (Condon et al. 1982). The extended LINER spectrum of the diffuse, ionized gas (Heckman, Armus and Miley 1987) might even seem to support this view (however, see below). The non-thermal nature of these compact sources has been confirmed by more recent optical, infrared and radio observations (Keel, this conference; Eales et al. 1988; Neff 1990, personal communication). Interestingly, the luminous "spur" has some of the characteristics of a Seyfert-like, narrow line region. It is aligned roughly with the axis of the double radio source and displays broad lines (~300 km s^{-1} FWHM) with blue wings up to 10 kpc from the galactic nucleus. If the extinction towards the nucleus is indicated by the strength of the Bγ line (Depoy et al. 1986), the SW spur has a corrected luminosity of $L_{H\alpha} \sim 2 \times 10^{42}$ erg s^{-1} which is comparable to that observed in luminous Seyfert 1 galaxies.

Evidence for transience. The kinematic data indicate the presence of two dynamical systems, closely spaced in velocity and position, that are almost perpendicular to each other. A more detailed study suggests that Axis 2 is

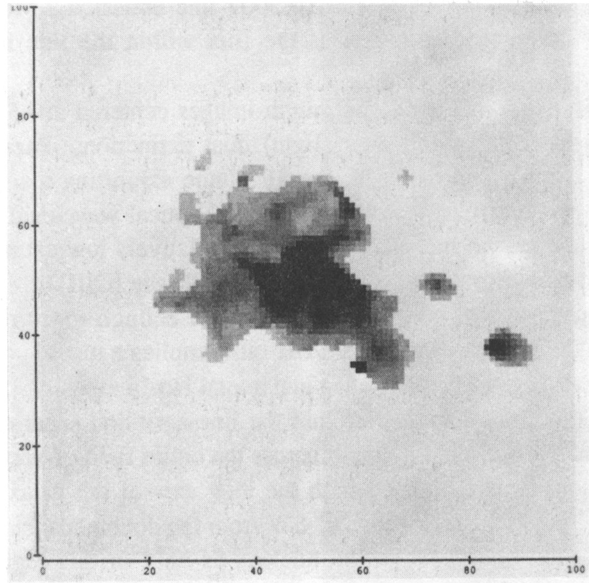

Figure 3(a). The Hα line flux over the inner 43" × 43" of NGC 6240 obtained from integrating over the HIFI line profiles. Only values that exceed a surface brightness of 2.5×10^{-16} erg cm^{-2} s^{-1} $arcsec^{-2}$ are shown. The darkest regions correspond to a surface brightness that is 5 magnitudes larger than the adopted cut-off. The brighter of the double nuclei occurs at pixel position (52,50); two bright HII regions are seen west of the nucleus at pixel positions (74,51) and (85,62).

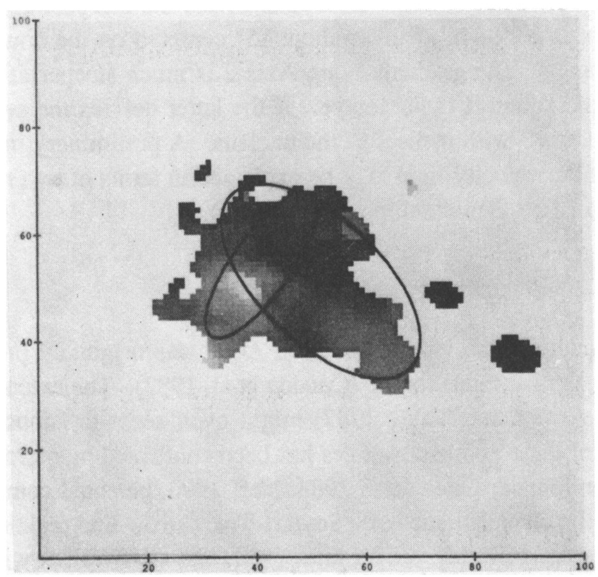

Figure 3(b). The Hα velocity field obtained from gaussian fits to the brightest component in the Hα line profiles. The velocities are shown only for those line profiles whose integrated surface brightness exceeds the cut-off used in Fig. 3(a). The lightest and darkest regions correspond to maximum velocities of -300 kms and 300 kms with respect to the velocity of the double nucleus. The two HII regions to the west are highly redshifted with respect to the nuclear velocity.

https://doi.org/10.1017/S0252921100005480 Published online by Cambridge University Press

the dense core of a disc that has been disrupted, while Axis 1 defines the major axis of a system that is undergoing coalescence with the second system. Dynamical simulations (Hernquist 1990, personal communication) show that these systems will be merged completely on a dynamical timescale (< 10^8 years).

Evidence for large-scale shocks. Harwit and collaborators (Harwit et al. 1986; Harwit and Fuller 1988) have shown how the kinetic energy release from two colliding galaxies can give rise to large-scale shocks which subsequently heat the dust grains. The line flux arising from the ram pressure in the shocks is proportional to V_S^n, where V_S is the relative velocity of impact, and n (≈3) and depends on many factors. Both optical (Fosbury and Wall 1979; Fried and Schulz 1983) and molecular spectroscopy (Lester, Harvey and Carr 1988) seem to indicate that shocked gas is present. It is tempting to suggest that the line flux – line width relation and the structure of the dust bands are somehow connected to the existence of large-scale shocks. In this event, we would expect to observe a line width – line excitation dependence in this region.

Evidence for a massive starburst. Of the suggested mechanisms, we favor a model in which the merger has triggered an episode of vigorous star formation. When two gas sheets are compressed at speeds of ~500 km s^{-1}, the onset of instabilities will generate large dense clumps which supersede star formation. The evidence for a wind-blown bubble supports the view of Heckman, Armus and Miley (1987) who suggest that the LINER spectrum of the ionized gas arises in shocks powered by starburst-driven winds. These authors find from a few long-slit positions that the ionized gas is overpressured with respect to the gravitational potential. The tenfold increase in the size of the putative nebula compared with M82 may reflect a similar increase in the supernova rate (Draine and Woods 1989). The main objection to the starburst picture has been the paucity of ionizing photons (Depoy et al. 1986) and the strength of the CO bands (Lester, Harvey and Carr 1988) which require a peculiar initial mass function. However, an evolved dense starburst produces many supernova remnants which, in our own galaxy, are strong sources of molecular hydrogen (Oliva and Moorwood 1988). In this case, a post-starburst phase could have only a few hot stars and radiate large amounts of H_2 and [Fe II] line emission.

Acknowledgments

JBH and RBT acknowledge the support of NSF grant AST 88-18900 and discussions with Martin Harwit, Lars Hernquist and Jon Weisheit.

References

Bland, J. and Tully, R. B. 1988, *Nature* **334**, 43.
Bland, J. and Tully, R. B. 1989, *Astron. J.* **98**, 723.
Condon, J. J. et al. 1982, *Ap. J.* **252**, 102.
Depoy, D., Becklin, E. E. and Wynn-Williams, C. G. 1986, *Ap. J.* **307**, 116.
Draine, B. T. and Woods, D. T. 1989, *Ap. J.*, preprint.
Eales, S. A. et al. 1988, *Infrared Arrays*, p. 345, eds. C. G. Wynn-Williams and E. E. Becklin.
Fosbury, R. A. E. and Wall, J. V. 1979, *MNRAS* **189**, 79.
Fried, J. W. and Schulz, H. 1983, *Astr. Ap.* **118**, 166.
Harwit, M. et al. 1986, *Ap. J.* **315**, 28.
Harwit, M. and Fuller, C. E. 198, *Ap. J.* **328**, 111.
Heckman, T. M., Armus, L. and Miley, G. K. 1987, *Astron. J.* **92**, 276.
Joseph, R. D., Wright, G. S. and Wade, R. 1984, *Nature* **311**, 132.
Lester, D. F., Harvey, P. M. and Carr, J. 1988, *Ap. J.* **329**, 641.
Oliva and Moorwood 1988, *Astr. Ap.*, preprint.
Rieke, G. H. et al. 1985, *Ap. J.* **290**, 116.